Life History of the Diatom *Schizostauron trachyderma*: Cell Size and Lipid Accumulation

Ewa Górecka[1]*, Przemysław Dąbek[1], Nikolai Davidovich[1,2], Olga Davidovich[2], Réjean Tremblay[3], Claude Belzile[3], Romain Gastineau[1] and Andrzej Witkowski[1]

[1] Institute of Marine and Environmental Sciences, University of Szczecin, Szczecin, Poland, [2] Karadag Scientific Station – Nature Reserve, Russian Academy of Science, Kurortnoe, Russia, [3] Institut des Sciences de la Mer de Rimouski, Université du Québec à Rimouski, Rimouski, QC, Canada

The focus of this study was to determine the mating type of *Schizostauron trachyderma* and examine the relationship between cell size (life cycle), lipid droplet size, and lipid content among diatoms with similar cell dimensions. To accomplish that, we have chosen monoclonal cultures of two closely related diatom species, namely *S. trachyderma* and *S. rawaii*. In a series of experiments, we successfully induced sexual reproduction within *S. trachyderma* strains to reconstruct the whole cell cycle involving cells of the maximum (initial cells) and minimum viable size for a given species. The mating-type and sexual reproduction stages were described and documented. A unique experimental setting involved initial cell isolation and their lipid droplet examination using flow cytometry and confocal microscopy after Nile Red staining. The results of the series of experiments indicate correlations between cell size, the number of neutral lipids per cell, and the size of lipid droplets, suggesting that cell capacity for lipid accumulation is dependent on their position in the life cycle.

Keywords: life cycle, sexual reproduction, auxosporulation, lipid droplets, Nile Red

INTRODUCTION

Diatoms (Bacillariophyceae) are eukaryotic, single-cell photosynthetic microalgae that can be found in every aquatic ecosystem. They generally play a key role in the global oxygen, carbon, and silica cycles in aquatic ecosystems and are one of the most important primary producers in the oceans (MacIntyre et al., 1996; Falkowski et al., 1998; Field et al., 1998; Smol and Stoermer, 2010). Marine benthic diatoms, as part of microphytobenthos, belong to the major group that micrograzers and higher trophic level communities from the most productive coastal systems seem to sustain on (Falkowski and Woodhead, 1992) due to the valuable lipids accumulated by diatoms as storage material. For this reason, the lipid content of the diatomaceous cell is grazed by herbivorous protists (Sherr and Sherr, 2007), invertebrates (Kelly and Scheibling, 2012), as well as vertebrates, e.g., fish (Gardner et al., 1990). The importance of diatoms in shallow benthic habitats has been studied recently by Cox et al. (2020), and the contribution of diatoms has been estimated to exceed 80%.

In the vast majority, the diatom interior protoplast is surrounded by a solid siliceous cell wall of various shapes and ornamentation known as the frustule. A diatom frustule consists of two valves (a bigger epivalve and a smaller hypovalve) connected by the girdle composed of band-like elements.

Frustule morphology and its spatial pattern strongly vary and are important tools for taxonomy. In general, the diatom life cycle consists of two phases, namely, asexual and sexual. The first phase corresponds to a period of vegetative multiplication (asexual division). As a result of mitotic division, each newly produced valve is a hypovalve. Among most diatom species, this leads to mean cell size diminution in the population (MacDonald, 1869; Pfitzer, 1869), and the maximum size of cells in a population is restored by auxosporulation followed by initial cell development. Normally, cell size restoration is achieved as a result of sexual reproduction, but vegetative enlargement has also been observed in some cases (Geitler, 1935; Round et al., 1990; Mann, 1993, 2011; Chepurnov and Roshchin, 1995; Kaczmarska et al., 2013).

Among diatoms, the lipids are the primary storage material, containing valuable neutral lipids [triacylglycerides (TAGs)], which contain potentially 20–60% of the total lipid content, depending on the species (Chen, 2012). The total lipid content has been studied among numerous species of diatoms (Chuecas and Riley, 1969; Pernet et al., 2003; Zheng et al., 2005), in the context of nutrient depletion (McGinnis et al., 1997; Renaud et al., 2002; Mohan et al., 2012; Adams and Bugbee, 2014) and salinity or light stress (Geider et al., 1985; Natana Murugaraj and Jeyachandran, 2007). The maximum lipid potential of diatom is considered species-specific and a heritable evolutionary trait (Fields and Kociolek, 2015). These authors discussed that the shape of the cell is irrelevant to the amount of produced lipids, whereas Graham et al. (2012) stated that cylindrical cells have a bigger potential to store lipids than fusiform-shaped cells due to their larger volume. Additionally, according to the theoretical model of microalgal growth for diatoms (Geider et al., 1986), the growth rate will decrease with an increase in cell size, which means that the decrease in cell number in population is compensated with cell size. Size-dependent lipid production was presented by Hitchcock (1982), but available data do not consider the comparison between different sized clonal cultures of the same species.

First, this study aimed to induce the sexual reproduction process and determine the mating type of monoraphid *Schizostauron trachyderma* (F. Meister) Górecka, Riaux-Gobin and Witkowski. Diatom mating-type classification, introduced by Geitler (1935, 1973), is based on the number, behavior, and morphology of gametes, as well as the mechanism of gamete fusion and auxospore formation. Understanding the reproductive biology of diatoms is key in recognizing diversification and speciation. One advantage of sexual reproduction characterization is the determination of maximum size range and cardinal points of the frustule, considered to be the diagnostic feature to a species and should be determined for each described taxon when possible (Edlund and Stoermer, 1997). Second, we aimed at the examination of the relationship between the cell size (the position in the life cycle) and the cell capacity to store lipids. To do so, cells of different sizes were necessary, but not different in terms of shape and evolutionary adaptation, hence same species monocultures were essential.

Inducing sexual reproduction in diatoms is a complex process. In the natural environment, it occurs spontaneously, but in the laboratory, various conditions must be fulfilled, e.g., specific for a species physicochemical parameters and appropriate cell size, below the size threshold, where diatoms gain the ability to reproduce sexually. Successful sexual reproduction and isolation of big, initial cells provided a unique opportunity to conduct size-related experiments. Accordingly, the experiment was prepared so that most factors that are variable at genus-level comparisons of lipid production in diatoms were decreased to a minimum.

This is the first experiment of this kind performed thus far. To accomplish reliable comparison, four clones of *S. trachyderma* and one clone of closely related *S. rawaii* Górecka, Ashworth, Sabir and Witkowski (Górecka et al., 2021) differing by their cell size were studied using flow cytometry and laser scanning microscopy. *Schizostauron* is a monoraphid marine benthic diatom genus; both *S. trachyderma* and *S. rawaii* possess a frustule of oval outline and relatively flat valve surface (one valve is slightly concave, and the second is slightly convex). Moreover, both species have similar morphological features, e.g., stauros, striae pattern on both valves, raphe endings, and acute apices. The difference between those species is the striae density and the size dimensions, *S. rawaii* is bigger than *S. trachyderma*. The close evolutionary relationship was confirmed with DNA sequences data in Górecka et al. (2021). The choice of those species was determined by clear taxonomic position, well-documented morphology and ultrastructure, and oval easy-to-estimate shape.

MATERIALS AND METHODS

Strain Origin
The monoclonal diatom cultures of *S. trachyderma* and *S. rawaii* were isolated from samples collected in Saudi Arabian littoral zone close to Jeddah. Both species are closely related and are similar in valve morphology, but different in length and width (Górecka et al., 2021). Strains from Szczecin Diatom Culture Collection (SZCZ) E1420–E1425 and E1428 were isolated from the sample collected on February 22, 2015, from the coral reef at 12 m depth (21.7561°N 39.05°E), and strains SZCZ E1426–E1427 were derived from samples collected on February 24, 2015, from the sand on a rock wall (22.8333°N 38.9°E). Strain SZCZ E1768 was derived from an initial cell isolated from an auxosporulating mixture of SZCZ E1420 and E1426. Strains are deposited in the SZCZ at the University of Szczecin, Poland. The full list of strains mentioned in this study is presented in **Table 1**.

Light Microscopy and Scanning Electron Microscopy
To prepare microphotographs of post-auxosporulation samples using scanning electron microscopy (SEM), the material was harvested and gently rinsed 7–10 times with distilled water to remove salts and to avoid destruction of organic components of frustule such as perizonium. The material was then pipetted onto the Whatman Nuclepore polycarbonate membrane filter with 5 µm pores (cat. no. 110613, Whatman, Maidstone, United Kingdom), mounted onto aluminum stubs, and coated with a 15 nm layer of gold-palladium alloy. The coatings were obtained using the magnetron sputtering method with the use of magnetron coater (Q150T, Quorum Technologies, Lewes,

TABLE 1 | List of *Schizostauron* spp. strains used for mating and lipid experiments.

Species	Strains	Length (μm)*	Width (μm)*	Cells type	Mating experiments	Lipid experiments
Schizostauron trachyderma	SZCZ E1420	23.45 ± 1.81 ($N = 20$)	14.03 ± 1.00 ($N = 20$)	Vegetative	✓	✓
Schizostauron trachyderma	SZCZ E1421	27.28 ± 0.83 ($N = 20$)	14.39 ± 0.45 ($N = 20$)	Vegetative	✓	✓
Schizostauron trachyderma	SZCZ E1422	24.72 ± 0.59 ($N = 20$)	13.55 ± 0.71 ($N = 20$)	Vegetative	✓	
Schizostauron rawaii	SZCZ E1423	37.24 ± 0.99 ($N = 20$)	23.27 ± 1.13 ($N = 20$)	Vegetative	✓	
Schizostauron rawaii	SZCZ E1424	41.12 ± 1.20 ($N = 20$)	23.81 ± 1.69 ($N = 20$)	Vegetative	✓	
Schizostauron rawaii	SZCZ E1425	38.45 ± 0.71 ($N = 20$)	23.93 ± 0.57 ($N = 20$)	Vegetative	✓	✓
Schizostauron trachyderma	SZCZ E1426	26.79 ± 0.73 ($N = 20$)	$14,76 \pm 0,44$ ($N = 20$)	Vegetative	✓	
Schizostauron trachyderma	SZCZ E1427	26.24 ± 0.61 ($N = 20$)	$14,15 \pm 0,71$ ($N = 20$)	Vegetative	✓	✓
Schizostauron trachyderma	SZCZ E1428	27.15 ± 0.82 ($N = 20$)	$14,88 \pm 0,53$ ($N = 20$)	Vegetative	✓	
Schizostauron trachyderma	SZCZ E1427 × SZCZ E1422	45.20 ± 2.77 ($N = 5$)	16.77 ± 0.54 ($N = 5$)	Initial		
Schizostauron trachyderma	SZCZ E1420 × SZCZ E1422	47.73 ± 1.81 ($N = 7$)	22.22 ± 1.82 ($N = 7$)	Initial		
Schizostauron trachyderma	SZCZ E1420 × SZCZ E1426	48.90 ± 2.14 ($N = 12$)	21.26 ± 1.32 ($N = 12$)	Initial		
Schizostauron trachyderma	SZCZ E1768	–	–	Post-initial		✓

*Cells were measured during mating experiments in September 2015.

United Kingdom) equipped with a turbomolecular pump. The thickness of the conductive films was monitored using quartz balance, which enables 0.1 nm measurement resolution. SEM observations were performed using Hitachi SU8020 (Hitachi, Tokyo, Japan) at the Faculty of Chemical Technology and Engineering, the Western Pomeranian University of Technology in Szczecin (Poland). Microphotographs of living cells were prepared by pipetting living cultures onto glass slides. Light microscopy (LM) documentation was obtained at the University of Szczecin with Zeiss Axio Scope A1 (Carl Zeiss, Jena, Germany) with an oil immersion lens (Zeiss PlanApochromat 100×) using a Canon EOS 500D camera with the Canon EOS Utility software (Canon, Tokyo, Japan). All measurements of diatom cells were performed using ImageJ software (Schneider et al., 2012).

Culture Conditions and Mating Experiment Details

Monoclonal cultures were established at the SZCZ using an inverted light microscope Nikon Eclipse TS100 (Nikon, Tokyo, Japan) equipped with magnification lens 4×, 10×, and 40× and glass micropipettes. Single cells were inoculated into plastic Petri dishes with f/2 medium (Guillard, 1975). Strains were kept in a growth chamber (Biogenet, Józefów, Poland) with radiation [photosynthetically active radiation (PAR), 400–700 nm] of 100 μmol photons m^{-2} s^{-1}, a 12 h photoperiod and a temperature of 20°C. Before mating, cultures were reinoculated periodically to maintain an exponential growth phase.

Mating experiments methodology applied for *S. trachyderma* follows Davidovich et al. (2017). Before the mating experiments, strains were checked daily under LM for homothallic reproduction (sexual reproduction within a clone). To conduct mating experiments, approximately 1 ml of suspended diatom mixture from each monoclonal culture was paired with another monoclonal culture in separate Petri dishes and then observed daily using an inverted light microscope with the 40× magnification objective. Several big cells resulting from sexual reproduction (initial cells) were isolated to establish monoclonal cultures. Terminology concerning sexual reproduction and auxosporulation follows the methods described by Kaczmarska et al. (2013).

Growth Rate Calculation and Lipid Droplet Measurements

For calculating the growth rate and doubling time, five strains were chosen: *S. trachyderma* (SZCZ E1420, E1421, E1427, and E1768) and *S. rawaii* (SZCZ E1425). Before the experiment, cultures were maintained in the exponential growth phase. For the experiment, 9 ml of each diatom strain was inoculated as three replicates into a 250 ml autoclaved Erlenmeyer flask with 80 ml of f/2 medium. Batch cultures were kept in a growth chamber with PAR of 100 μmol photons m^{-2} s^{-1} at 20°C and 12 h photoperiod. The cells were counted every second day using the Malassez counting chamber for 13 days. Before cell count, the cultures were mixed gently to detach the diatoms growing on the bottom of the flask. Growth rate and doubling time were calculated following the methods described by Wood et al. (2005).

The same strains were chosen for lipid droplet measurements. Flow cytometry analysis and confocal laser scanning microscopy visualization were conducted at the Institut des Sciences de la Mer de Rimouski at UQAR in Quebec, Canada. For both analyses, cells were stained with Nile Red (cat. no. N3013, Sigma Aldrich, St. Louis, MO, United States) following the method suggested by Greenspan et al. (1985).

Each strain was divided into batch cultures in standard f/2 medium (with modification of nitrogen, half with 1,100 μM/L $NaNO_3$ and half with 660 μM/L $NaNO_3$, the non-modified medium contains 880 μM/L

NaNO$_3$) in triplicates and kept in the same light and temperature conditions as for the growth rate experiment. After days 13 and 14, the cultures were harvested and stained.

Cell abundance, Nile Red fluorescence, and cell size were measured using a CytoFLEX (Beckman Coulter, Brea, CA, United States) flow cytometer. Each culture was analyzed on two consecutive days (days 13 and 14). The blue laser (488 nm) was used to measure forward scatter, side scatter, orange fluorescence from Nile Red-neutral lipid complexes (585/42 nm BP), and red fluorescence from chlorophyll (690/50 nm BP). Before the analysis, samples were strained on a 35 µm Nylon mesh to remove most chains of cells. Polystyrene microspheres of 2 µm diameter (Fluoresbrite YG, Polysciences) were added to each sample as an internal standard and to standardize the cell size and fluorescence. Cell size, expressed as spherical equivalent diameter, was estimated from a forward scatter calibration using algal cultures for which the length and width of the cell were measured using LM.

Nile Red stained samples were also observed using an LSM700 (Carl Zeiss) laser scanning confocal microscope at a 400 × magnification. ZEN 2009 software was used to collect images of Nile Red fluorescence (excitation at 488 nm) and chlorophyll *a* fluorescence (excitation at 639 nm). The lipid droplets in 12–42 cells of each strain were measured on day 14 from one triplicate of each strain. The lipid bodies were treated as two-dimensional circular objects to estimate their total area per cell and compared with flow cytometry results. The lipid droplets of diatoms in valve face view only were considered for measurements. Some cells had a single drop of lipids, and some cells had multiple. In such a case, the area of all droplets was summed up.

Statistical Analysis

Pearson correlation coefficients and *p*-values were calculated, and the graphs were plotted using the *R* software (R Core Team, 2020). Value of $p < 0.05$ was considered significant. To check the variability of the datasets, the Kruskal-Wallis test was performed using the Tukey *post hoc* test with Past software (Hammer et al., 2001).

RESULTS

Schizostauron trachyderma Life Cycle
Breeding Behavior and Life Cycle

Successful sexual reproduction was observed in the mixture of five sexually compatible monoclonal cultures isolated from Saudi Arabia (SZCZ E1420, E1421, E1422, E1426, and E1427). No homothallic reproduction was observed. Clones SZCZ E1422 and SZCZ E1426 engaged in sexual reproduction with clones representing the opposite mating types, namely, SZCZ E1420, SZCZ E1421, and SZCZ E1427. The average size of each strain is provided in **Table 1**, and the mating chart is provided in **Table 2**.

The beginning of the mating process consisted of the pairing of sexually compatible cells in the mixture. Two or more cells were grouped, connecting side by side to each other (**Figures 1A,D**), followed by the production of a mucilage envelope. Interaction and gamete exchange can be observed in a particular pair of cells that we regarded as gametangial pair. Each cell in a gametangial pair produced two gametes within 24 h of pairing (**Figures 1A,D**). In a gametangial pair, all four gametes presented a similar rounded shape, with only minor differences in size and shape within one cell (**Figures 1A,C**). Syngamy occurred in sequence, with one passive and one active gamete fusing crosswise, one pair after another (**Figures 1B–G**) within 10–15 min from the beginning of gamete migration. Fused gametes were usually located diagonally to each other. As a result, two spherical zygotes were formed (**Figures 1C,H,I**), their bipolar expansion started within a few tens of minutes (**Figure 1J**). After ca. 12 h, elongated, fully grown auxospores were built (**Figure 1K**), finally resulting in the development of initial cells (cf. SEM **Figure 2**). Except for the mucilage envelope, no other organic compounds accompanying auxosporulation were observed by LM, with the remains of the perizonium only observable using SEM (**Figure 2**). The post-initial cells were isolated and included in the SZCZ under the numbers E1429, E1766–1768.

During the life cycle, the valve length varied between 19 µm (the smallest vegetative cell observed) and 51 µm (initial cells), and the valve width varied between 11 and 25 µm. The changes in width were not proportional to the changes in length. Initial and post-initial cells were more elongated in comparison to smaller,

TABLE 2 | Results of mating experiments of *Schizostauron* spp.

Species	Mating type	Strain SZCZ	E1420	E1421	E1422	E1423	E1424	E1425	E1426	E1427	E1428
S. trachyderma	+	E1420	/								
S. trachyderma	+	E1421	0	/							
S. trachyderma	−	E1422	1	0	/						
S. rawaii	unk.	E1423	0	0	×	/					
S. rawaii	unk.	E1424	0	×	0	×	/				
S. rawaii	unk.	E1425	0	0	×	×	×	/			
S. trachyderma	−	E1426	1	1	0	0	0	0	/		
S. trachyderma	+	E1427	0	0	1	×	0	×	1	/	
S. trachyderma	unk.	E1428	×	×	0	×	×	×	0	0	/

0, sexual reproduction not observed in mixed culture; 1, sexual reproduction occurred in mixed culture; /, no homothallic reproduction observed; ×, cross not tested; unk., mating type unknown.
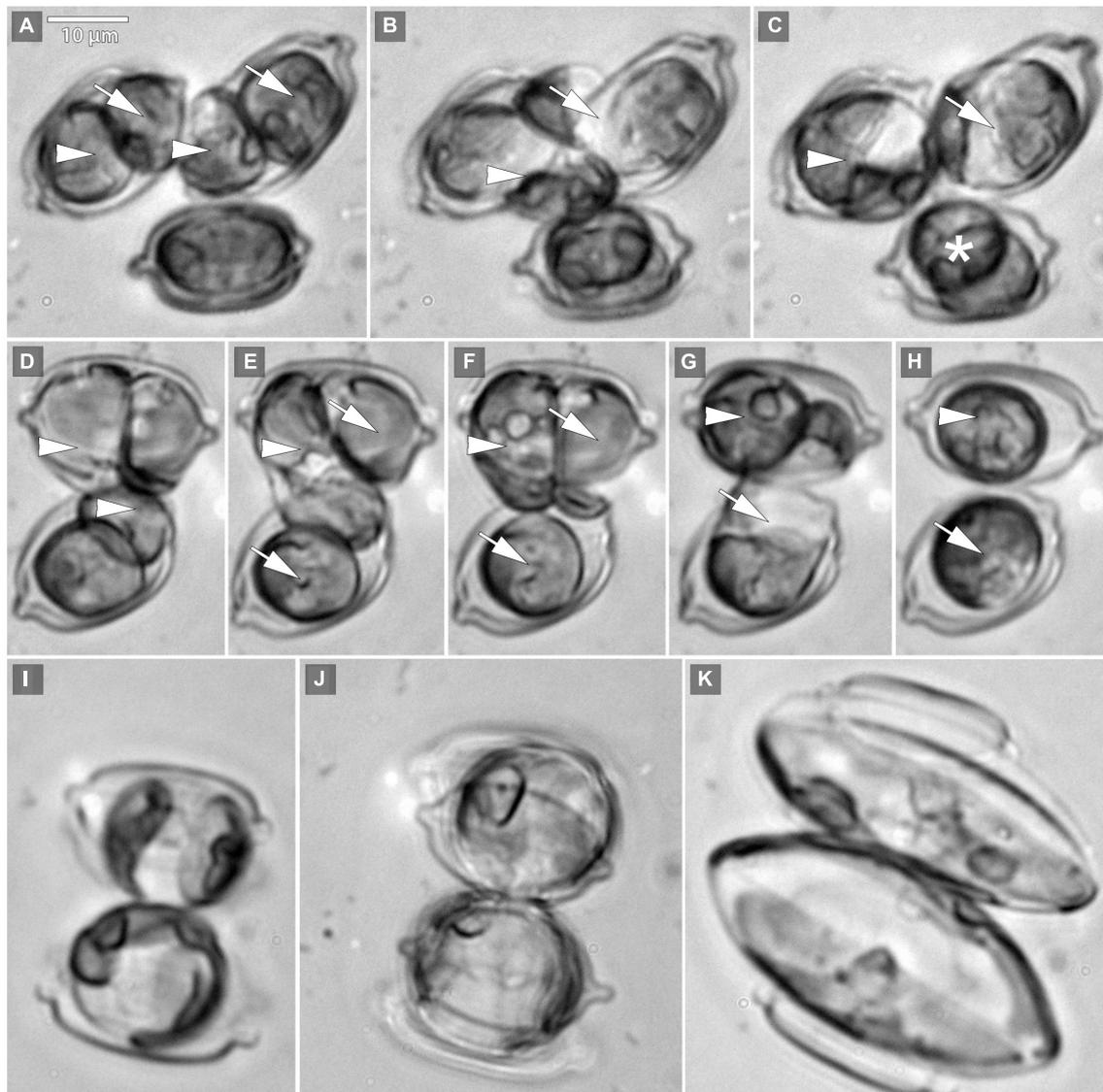
FIGURE 1 | Microphotographs of *Schizostauron trachyderma* auxosporulation using light microscopy (LM). **(A)** Two pairs of gametes formed within a gametangial cell (arrowheads mark pair 1, arrows mark pair 2). **(B)** Gametes simultaneously fuse crosswise (arrowhead marks pair 1, arrow marks pair 2). **(C,H)** Zygotes (arrows and arrowheads) and gametes of an unpaired cell (asterisk) that will not reproduce successfully. **(D–G)** Two pairs of gametes (arrowheads mark pair 1, arrows mark pair 2), fusing crosswise, consequently. **(I–K)** Two growing auxospores.

more rounded vegetative cells. Sexual reproduction was observed in pairs of monoclonal cultures that did not exceed 29 μm in length. As a result of successful auxosporulation, the population restored its maximum, species-specific size, which was more or less two times bigger than the parental cells.

Growth and Size of the Cells and Lipid Droplets

The growth rate was significantly different between strains. The highest growth rate (0.31 day^{-1}) was obtained by strain E1427 (*S. trachyderma*). Strain E1421 reached the highest value for doubling time (6.8 days) with the lowest growth rate (0.10 day^{-1}).

The strain with the biggest cells of *S. trachyderma*, SZCZ E1768 (N = 20, 34.1 μm) reached a growth rate of 0.2 days^{-1} and a doubling time of 3.5 days. The growth rate of strain of the bigger species, *S. rawaii* with the mean cell length of strain E1425 (N = 20, 35.0 μm) was similar to strains with the biggest cells of *S. trachyderma* E1768 (growth rate 0.25 days^{-1} and doubling time 2.8 days). The mean cell length of each strain examined is presented in **Table 3**. The growth curves are presented in **Figure 3**.

The relative neutral lipid fluorescence was significantly different between the strains. The fluorescence of neutral lipids measured on day 14 was higher in strains E1420, E1425, E1427, and E1768 than measured on day 13. In strain E1421, the
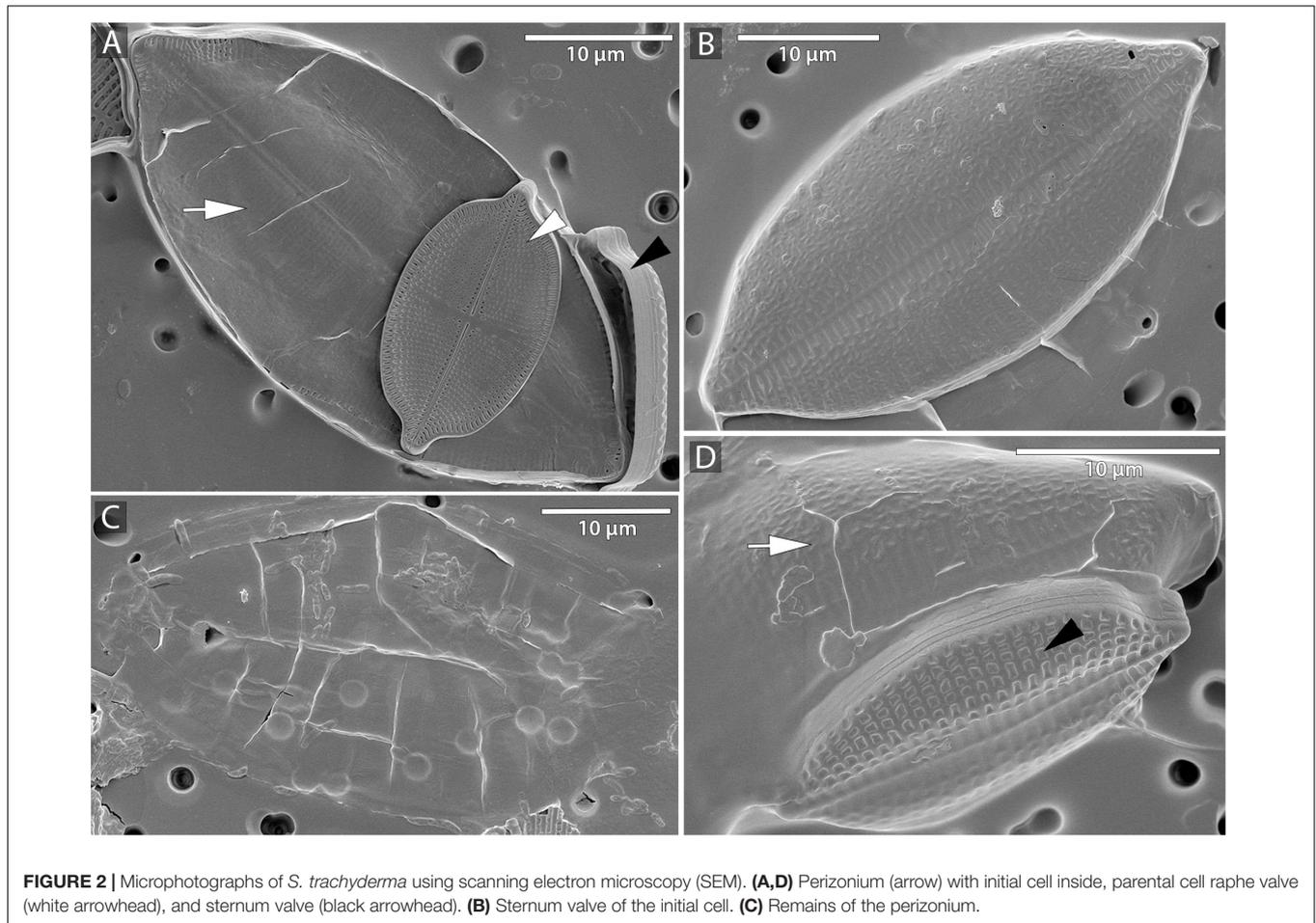
FIGURE 2 | Microphotographs of *S. trachyderma* using scanning electron microscopy (SEM). **(A,D)** Perizonium (arrow) with initial cell inside, parental cell raphe valve (white arrowhead), and sternum valve (black arrowhead). **(B)** Sternum valve of the initial cell. **(C)** Remains of the perizonium.

TABLE 3 | *Schizostauron* spp. strains parameters.

Strain SZCZ	Species	Average growth rate (Day^{-1})	Average doubling time (Day)	Mean cell length (μm) ($N = 20$)*	Mean lipid droplets area per cell (μm^2)
E1420	*Schizostauron trachyderma*	0.22 ± 0.03	3.2	24.1 ± 1.2	99.3 ± 44.8 ($N = 42$)
E1421	*Schizostauron trachyderma*	0.10 ± 0.03	6.8	24 ± 0.9	96.1 ± 48.5 ($N = 22$)
E1425	*Schizostauron rawaii*	0.25 ± 0.02	2.8	35 ± 0.7	216.8 ± 125.7 ($N = 15$)
E1427	*Schizostauron trachyderma*	0.31 ± 0.03	2.2	22.6 ± 0.8	73.6 ± 27.0 ($N = 17$)
E1768	*Schizostauron trachyderma*	0.20 ± 0.02	3.5	34.1 ± 1	372.9 ± 241.0 ($N = 12$)

Cells were measured during lipids experiments in April 2019.

fluorescence value was similar on both days. The highest values of neutral lipid fluorescence were measured in strain E1768 (post-initial cells of *S. trachyderma*) and strain E1425 (*S. rawaii*) on day 14. The lowest value of neutral lipid fluorescence was measured on day 13 in strain with the smallest cells of *S. trachyderma* E1427. On day 14, the lowest value was measured within the strain of *S. trachyderma* E1421 (**Figure 4**). **Figures 5A,B** shows the relationship between relative cell size and fluorescence of neutral lipids stained with the Nile Red for both nutrient replete and deplete pooled together, as there was no significant difference between treatments. The neutral lipid cellular content increased with increasing cell size in all cases with correlation coefficients >0.6 and value of $p < 0.05$ (**Figure 5**). The flow

cytometric profiles are provided for the smallest and the biggest strains of *S. trachyderma* in **Figures 6A–D**.

Confocal microscopy measurements are positively correlated with flow cytometry results and present a similar pattern, i.e., the area of lipid droplets in the cell images is larger in bigger cells and higher values of neutral lipid per cell are measured in strains with bigger cells (SZCZ E1768 and SZCZ E1425). The mean lipid droplet area in cells is presented in **Table 3**. The largest mean area was measured within the cell images from strain E1768 (372.9 μm^2) and strain E1425 (216.8 μm^2), the smallest mean area in the images of cells from strain E1427 (73.6 μm^2). Examples of confocal microscopy images that were used to measure the lipid droplets are presented in **Figure 7**.
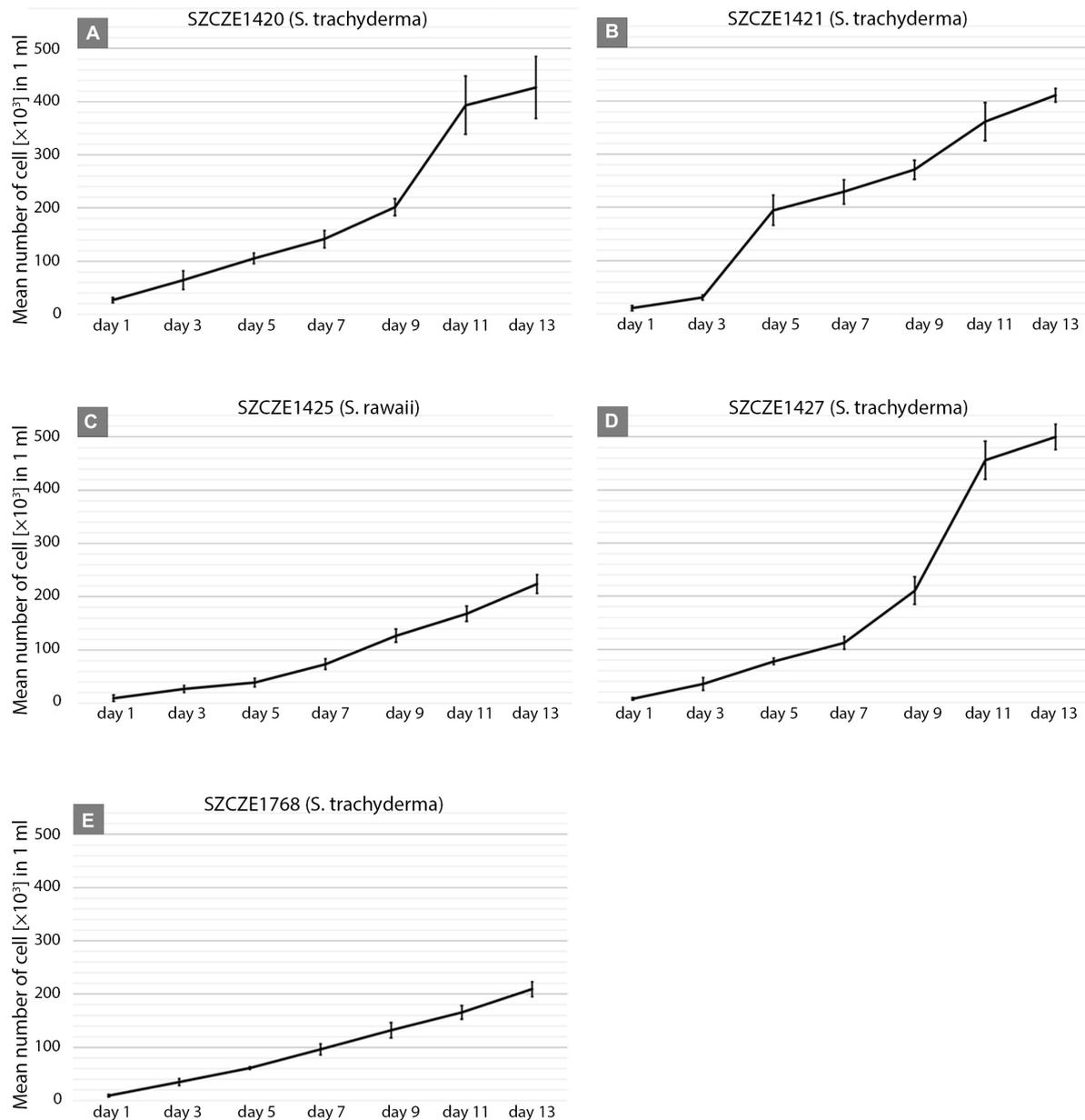
FIGURE 3 | (A–E) Growth curves of *Schizostauron* spp. strains, based on a mean value calculated from triplicates. Error bars represent standard deviations.

The data used to calculate statistical significance, difference, and correlations along with the results of these statistical analyses are presented in **Supplementary Data 1**.

DISCUSSION

Sexual Reproduction in *Schizostauron*

The life cycle of *Schizostauron* representative was first studied by Davidovich et al. (2017), where sexual reproduction was successfully documented for *S. kajotkei* Dąbek, Górecka and Witkowski (referenced as *Schizostauron* sp. 1). Mating

experiments presented here were successful only for *S. trachyderma* but not for *S. rawaii*. The results obtained for *S. trachyderma* are coherent with the aforementioned study. The pattern of sexual reproduction of *S. kajotkei* was determined as type I based on the classification presented by Geitler (1973), which implies the production of two gametes per gametangium and two auxospores per gametangial pair. However, the behavior of gametes for *S. kajotkei* remained unclear. For *S. trachyderma*, we observed a trans-anisogamous type of reproduction. Two morphologically equal but behaviorally different gametes were formed by each gametangium. The active gamete from one gametangium moved toward the passive gamete of the second

FIGURE 4 | The mean neutral lipid fluorescence in *Schizostauron* spp. strains measured using flow cytometer on day 13 (n = 6 cultures) and day 14 (n = 5 cultures) of the experiment. Error bars represent standard deviations.
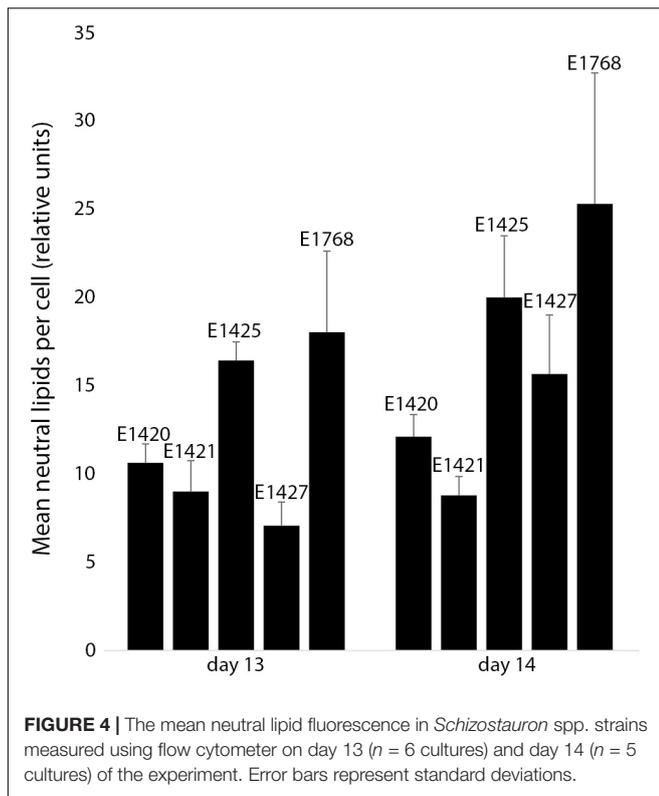
gametangium, but at the same time, the active gamete from the second gametangium was in opposite motion. As a result, there were two zygotes, each lying in the parental gametangial cell not between the opened frustules (being surrounded by four thecae), as in the case of strict isogamy.

The recent studies on the phylogenetic position of *Schizostauron* consistently suggest its close relationship to monoraphid genera such as *Astartiella*, *Madinithidium*, *Karayevia*, and *Kolbesia*, all nested in Stauroneidaceae family

clade and not related to other monoraphid genera such as *Achnanthes* or *Cocconeis* (Davidovich et al., 2017; Górecka et al., 2021). Our results describing characteristics of sexual reproduction in *S. trachyderma* support this, as *S. kajotkei* and *S. trachyderma* pattern of sexual reproduction shares similarities to *Craticula* spp. (two morphologically isogamous gametes, Mann and Stickle, 1991) and *Stauroneis phoenicenteron* (two isogamous gametes, Amato, 2010), but not to monoraphid forms such as *Cocconeis* spp. which matched Geitler's type II (one gamete per gametangium, Mizuno and Okuda, 1985; Mizuno, 1994). While the mating type is one of the characteristic features to distinguishing the diatom genera, it cannot be recommended as a primary diagnostic criterion, as unrelated diatoms may have similar reproductive strategies and currently only a few genera have their sexual reproduction thoroughly documented.

Lipid Droplet Size and Cell Capacity for Lipid Accumulation

In diatoms, the cell size and storage capabilities are restricted by the siliceous frustule, no matter under what stress the cultures would grow. Moreover, the cell size of most species is decreasing with time, unless an auxosporulation event occurs. This represents a challenge for the long-time, large-scale cultivation of marine benthic diatoms for biomass and secondary metabolite production. Sexual reproduction that could restore the cell size to the maximum has never been observed in monoclonal cultures of hitherto studied species of *Schizostauron*; moreover, apart from the sexual partner, favorable conditions and suitable phase of the life cycle are needed.

In the experiment, two nutrient regimes were applied: one with nitrogen limitation and the other with excess nitrogen. The statistical analysis indicated no significant difference between treatments; even though, according to the literature, nitrogen deprivation should influence the neutral lipid amount and the growth of the diatoms (Wu et al., 2014; Alipanah et al., 2015). Additionally, the cultures were in the exponential growth phase until the end of the experiment. These may imply that the

FIGURE 5 | Correlation plot of *Schizostauron* spp. cell sizes and neutral lipid fluorescence measured using flow cytometer on day 13 **(A)** and day 14 **(B)**.
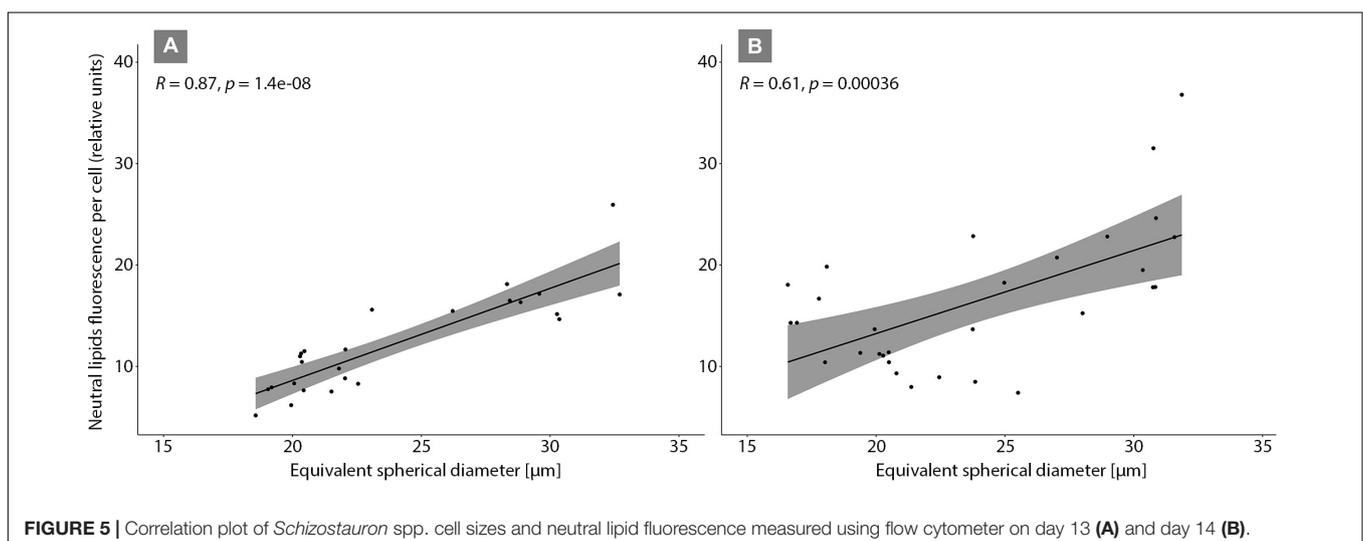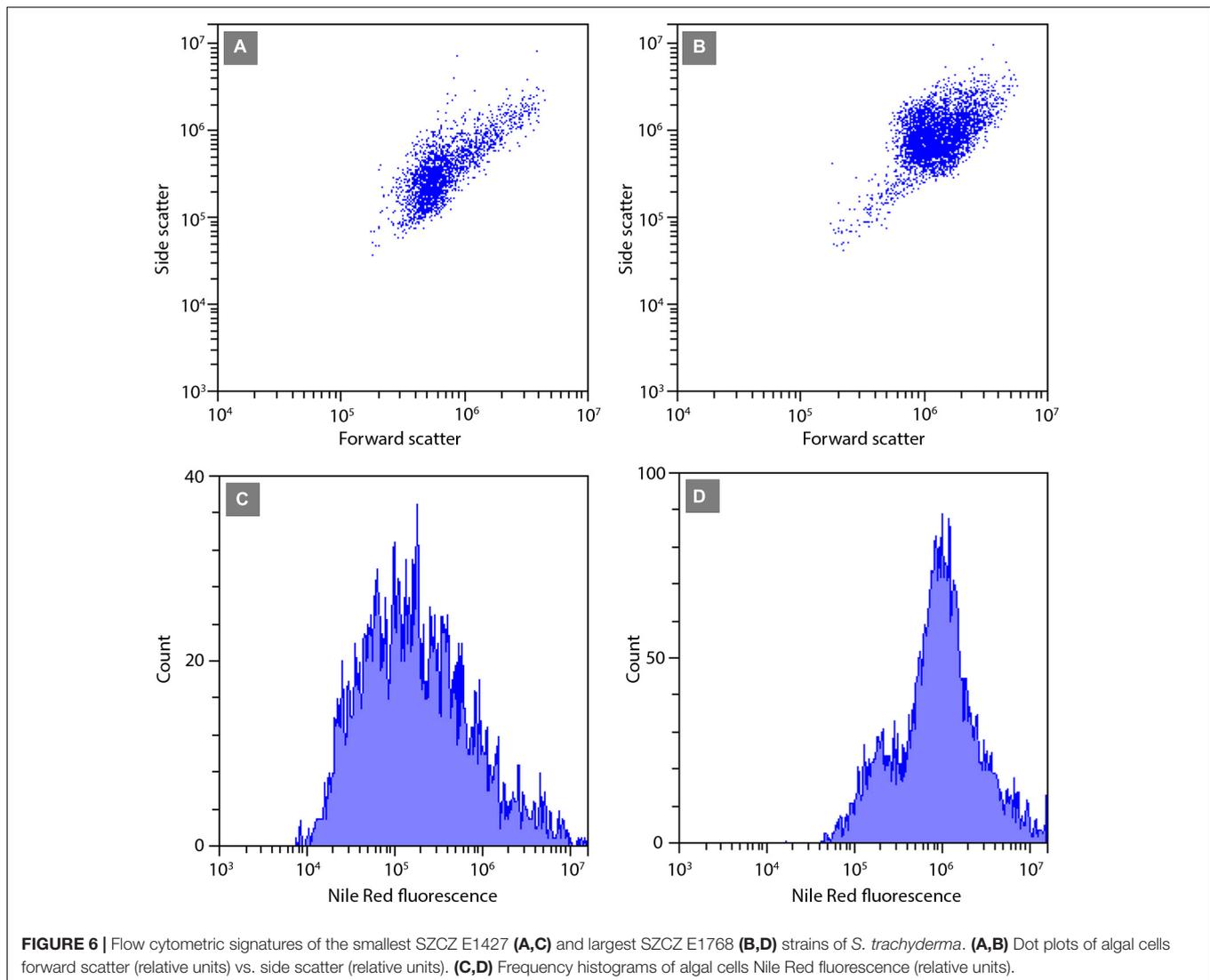
FIGURE 6 | Flow cytometric signatures of the smallest SZCZ E1427 **(A,C)** and largest SZCZ E1768 **(B,D)** strains of *S. trachyderma*. **(A,B)** Dot plots of algal cells forward scatter (relative units) vs. side scatter (relative units). **(C,D)** Frequency histograms of algal cells Nile Red fluorescence (relative units).

nitrogen was neither in excess nor in shortage, and the cultures did not reach biomass level high enough to consume all the nitrogen. Moreover, there was no statistical difference between the treatments. In light of the above, the results concerning these parameters were pooled together.

The choice of calculating lipid droplet area instead of their volume was dictated by the shape of the diatom, which we have chosen as the study object. The confocal images allowed us to see only two dimensions at a time. The frustule shape of both, *S. trachyderma* and *S. rawaii*, is oval in outline with a flat surface but rather narrow in girdle view. This caused the lipid droplets to become flattened in the "hidden" dimension (cf. **Figures 7B,D**) and wider in visible dimensions. With volume calculations, this would force a bigger assumption about the hidden dimension than with area calculations.

The correlation between cell length, lipid fluorescence, and lipid droplet projective area per cell (**Figures 4**, **5**) was tested using monoclonal strains of closely related species. We have chosen cells of various sizes, ranging from 24.0 to 35.0 μm

in length. The volume of cells is, in fact, changing during the life cycle, but generally, the most variable characteristic in pennate diatoms is the length of the cells (Round et al., 1990), which applies to the investigated *Schizostauron* species as well (Davidovich et al., 2017; Górecka et al., 2021).

The positive correlations between cell size and neutral lipids per cell (**Figure 5**) suggest that at least at a species level, the lipid accumulation is most likely size-dependent. This was also demonstrated by lipid droplet area measured using confocal microscopy where the bigger the cell, the bigger was the total projective area of lipid droplets. Nevertheless, for the tested strains, several factors stimulate the lipid content per cell, e.g., stressing conditions. Flow cytometry analysis, based on strains harvested on 2 consecutive days, shows results that differ from each other. As shown in **Figure 4**, the mean neutral lipid fluorescence per cell was larger on the second day of harvesting in almost every strain. The diatoms produce lipids as storage energy; therefore, the cells in stressing conditions at the end of the exponential growth

FIGURE 7 | Representative confocal microscope images showing lipid droplets, stained with the Nile Red (red channel) and chlorophyll (blue channel) in different strains of *Schizostauron* spp. **(A,B)** SZCZ E1420, **(C,D)** SZCZ E1421, **(E,F)** SZCZ E1425, **(G,H)** SZCZ E1427, **(I,J)** SZCZ E1768.
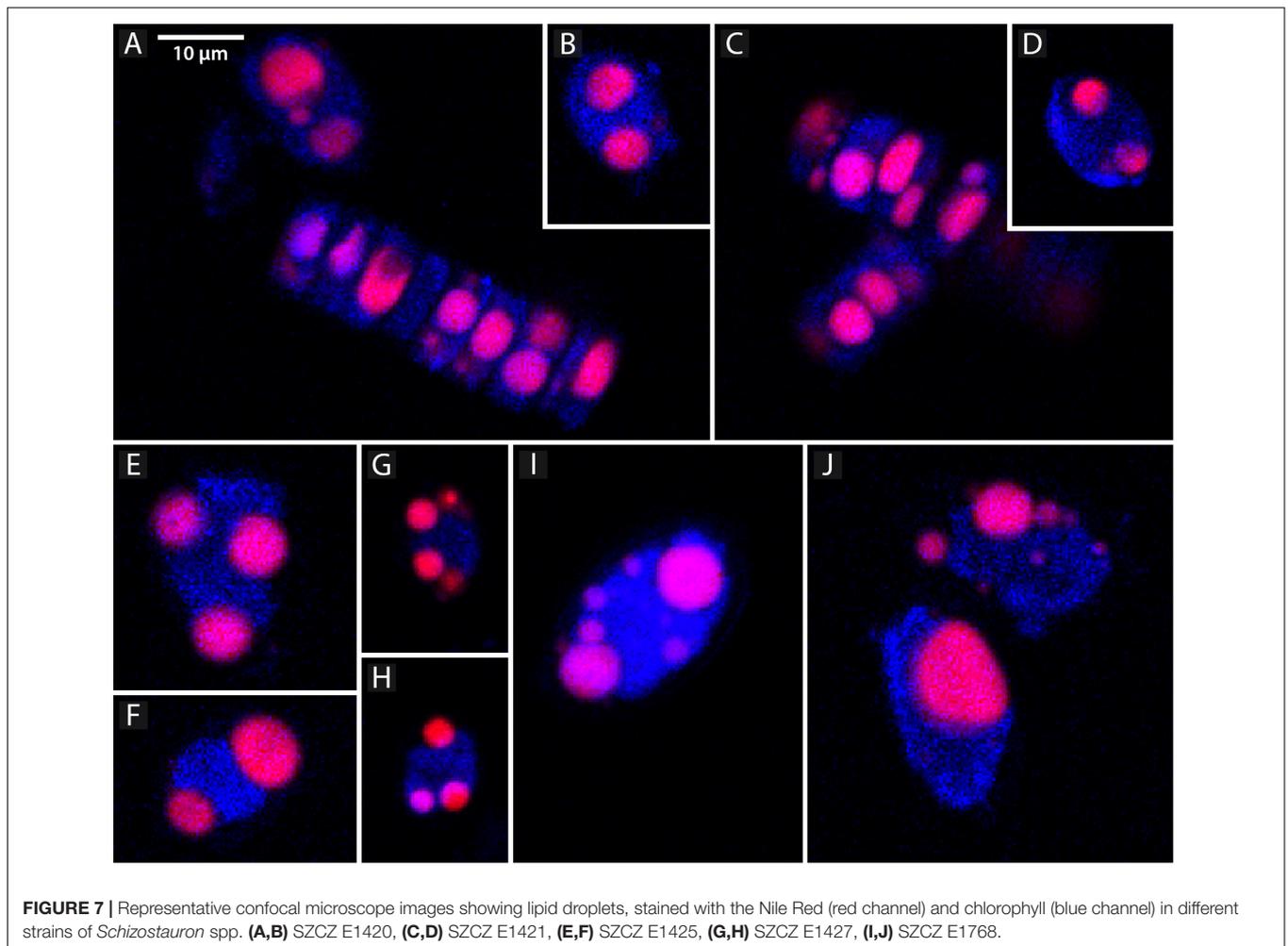
phase store more lipids (Geider et al., 1985; McGinnis et al., 1997; Renaud et al., 2002; Natana Murugaraj and Jeyachandran, 2007; Mohan et al., 2012; Adams and Bugbee, 2014). This is consistent with the results presented in **Figure 4**. Even though the values of lipid fluorescence were different on both days, the pattern is similar, the bigger cells of *Schizostauron* spp. are capable to store more lipids than the smaller cells (**Figure 5**).

This study aims to test whether the lipid storage capability varies during the life cycle in particular diatom species. It is worth mentioning that the maximum lipid production capability of *Schizostauron* spp. has not been assessed, but the relationship between cell size and lipid droplet size of *Schizostauron* spp. was calculated based on estimation. A similar study on the content of lipids in diatoms with different volumes is presented by Hitchcock (1982), but the results suggest the opposite relation. The study focused on various planktonic diatom species whose cell capacity and the total lipid amount were estimated based on the extracted material. The yield of oil extracted from microalgae may vary depending on species (Li et al., 2014; Gorgich et al., 2020; Svenning et al., 2020), and therefore, more precise methods should be applied to estimate the theoretical capacity and lipid

potential of the diatom cells. In contrast, the focus of our study was the variability of the lipid storage capability on the diatom species level, thus comparison between our results and results obtained for genus level studies is limited. To confirm the size-dependency of lipid accumulation, more studies are needed which must consider cultures of different sizes, but the same species, or at least species from the same evolutionary lineages.

To the best of our knowledge, this is the first experiment involving the study of neutral lipids along the whole cell cycle of the diatom monoclonal cultures. Describing and documenting the life cycle of *S. trachyderma* using a light microscope is a valuable input into understanding the biology of this genus and its relationship to other monoraphid genera. Moreover, successful sexual reproduction allowed us to test the correlation between cell size and neutral lipid storage. The estimation developed in our study supports the assumption that the volume of cells limits the capacity for lipid accumulation at a species level. This could be considered for optimal biomass production. Combining the choice of a lipid-rich evolutionary lineage with other criteria, such as fast growth or resistance to sudden changes in environmental conditions, should help to optimize cultivation and lipid production. Results of our experiments are a significant

contribution to the role that diatoms play in shallow marine benthic ecosystems, which largely sustain diatomaceous lipids serving the extremely diverse systems involving grazers from unicellular protists through invertebrates to benthic fish.

DATA AVAILABILITY STATEMENT

The raw data supporting the conclusions of this article are available in the **Supplementary Material**.

AUTHOR CONTRIBUTIONS

FUNDING

ACKNOWLEDGMENTS

SUPPLEMENTARY MATERIAL

The Supplementary Material for this article can be found online at: https://www.frontiersin.org/articles/10.3389/fmars.2021.793665/full#supplementary-material

REFERENCES

Adams, C., and Bugbee, B. (2014). Enhancing lipid production of the marine diatom *Chaetoceros gracilis*: synergistic interactions of sodium chloride and silicon. *J. Appl. Phycol.* 26, 1351–1357.

Alipanah, L., Rohloff, J., Winge, P., Bones, A. M., and Brembu, T. (2015). Whole-cell response to nitrogen deprivation in the diatom *Phaeodactylum tricornutum*. *J. Exp. Bot.* 66, 6281–6296. doi: 10.1093/jxb/erv340

Amato, A. (2010). Species concepts and definitions: reproductive isolation as a tool to reveal species boundaries. *Int. J. Plant Reprod. Biol.* 2, 114–126.

Chen, Y. C. (2012). The biomass and total lipid content and composition of twelve species of marine diatoms cultured under various environments. *Food Chem.* 131, 211–219.

Chepurnov, V. A., and Roshchin, A. M. (1995). Inbreeding influence on sexual reproduction of *Achnanthes longipes* Ag. (Bacillariophyta). *Diatom Res.* 10, 21–29. doi: 10.1080/0269249x.1995.9705327

Chuecas, L., and Riley, J. P. (1969). Component fatty acids of the total lipids of some marine phytoplankton. *J. Mar. Biol. Assoc. UK.* 49, 97–116. doi: 10.1017/s0025315400046439

Cox, T. E., Cebrian, J., Tabor, M., West, L., and Krause, J. W. (2020). Do diatoms dominate benthic production in shallow systems? *Limnol. Oceanogr.* 5, 425–434. doi: 10.1002/lol2.10167

Davidovich, N. A., Davidovich, O. I., Witkowski, A., Li, C. L., Dąbek, P., Mann, D. G., et al. (2017). Sexual reproduction in *Schizostauron* (Bacillariophyta) and a preliminary phylogeny of the genus. *Phycologia* 56, 77–93. doi: 10.2216/16-29.1

Edlund, M. B., and Stoermer, E. F. (1997). Ecological, evolutionary, and systematic significance of diatom life histories. *J. Phycol.* 33, 897–918. doi: 10.1111/j.0022-3646.1997.00897.x

Falkowski, P. G., Barber, R. T., and Smetacek, V. (1998). Biogeochemical controls and feedbacks on ocean primary production. *Science* 281, 200–206. doi: 10.1126/science.281.5374.200

Falkowski, P. G., and Woodhead, A. (1992). *Primary Productivity and Biogeochemical Cycles in the Sea. Environmental Science Research Volume*. New York, NY: Plenum, 42.

Field, C. B., Behrenfeld, M. J., Randerson, J. T., and Falkowski, P. G. (1998). Primary production of the biosphere: integrating terrestrial and oceanic components. *Science* 281, 237–240. doi: 10.1126/science.281.5374.237

Fields, F. J., and Kociolek, J. P. (2015). An evolutionary perspective on selecting high-lipid-content diatoms (Bacillariophyta). *J. Appl. Phycol.* 27, 2209–2220. doi: 10.1007/s10811-014-0505-1

Gardner, W. S., Quigley, M. A., Fahnenstiel, G. L., Scavia, D., and Frez, W. A. (1990). "Pontoporeia hoyi—a Direct Trophic Link between Spring Diatoms and Fish in Lake Michigan in Large Lakes. Brock/Springer Series," in *Contemporary Bioscience*, eds M. M. Tilzer and C. Serruya (Heidelberg: Springer), 632–644.

Geider, R. J., Osborne, B. A., and Raven, J. A. (1985). Light dependence of growth and photosynthesis on *Phaeodactylum tricornutum* (Bacillariophyceae). *J. Phycol.* 21, 609–619. doi: 10.1111/j.0022-3646.1985.00609.x

Geider, R. J., Platt, T., and Raven, J. A. (1986). Size dependence of growth and photosynthesis in diatoms: a synthesis. *Mar. Ecol. Prog. Ser.* 30, 93–104.

Geitler, L. (1935). Reproduction and life history in diatoms. *Bot. Rev.* 1, 149–161. doi: 10.1007/bf02870149

Geitler, L. (1973). Auxosporen bildung und Systematik bei pennaten Diatomeen und die Cytologie von Cocconeis-Sippen. *Osterr. Bot. Z.* 122, 299–321. doi: 10.1007/bf01376232

Górecka, E., Ashworth, M. P., Davidovich, N., Davidovich, O., Dąbek, P., Sabir, J. S. M., et al. (2021). Multigene phylogenetic data place monoraphid diatoms

Schizostauron and *Astartiella* along with other fistula bearing genera in the Stauroneidaceae. *J. Phycol.* 57, 1472–1491. doi: 10.1111/jpy.13192

Gorgich, M., Mata, T., Martins, A., Branco–Vieira, M., and Caetano, N. (2020). Comparison of different lipid extraction procedures applied to three microalgal species. *Energy Rep.* 6, 477–482. doi: 10.1016/j.egyr.2019.09.011

Graham, J. M., Graham, L. E., Zulkifly, S. B., Pfleger, B. F., Hoover, S. W., and Yoshitani, J. (2012). Freshwater diatoms as a source of lipids for biofuels. *J. Ind. Microbiol. Biotechnol.* 39, 419–428. doi: 10.1007/s10295-011-1041-5

Greenspan, P., Mayer, E. P., and Fowler, S. D. (1985). Nile Red: A selective Fluorescent Stain for Intracellular Lipid Droplets. *J. Cell Biol.* 100, 965–973. doi: 10.1083/jcb.100.3.965

Guillard, R. R. L. (1975). "Culture of phytoplankton for feeding marine invertebrates," in *Culture of Marine Invertebrate Animals*, eds W. L. Smith and M. H. Chanley (Boston, USA: Springer), 29–60. doi: 10.1007/978-1-4615-8714-9_3

Hammer, Ø, Harper, D. A. T., and Ryan, P. D. (2001). PAST: Paleontological Statistics Software Package for Education and Data Analysis. *Palaeontol. Electron* 4, 1–9.

Hitchcock, G. L. (1982). A comparative study of the size-dependent organic composition of marine diatoms and dinoflagellates. *J. Plankton Res.* 4, 363–377. doi: 10.1093/plankt/4.2.363

Kaczmarska, I., Poulíčková, A., Sato, S., Edlund, M. B., Idei, M., Watanabe, T., et al. (2013). Proposals for a terminology for diatom sexual reproduction, auxospores and resting stages. *Diatom Res.* 28, 263–294. doi: 10.1080/0269249x.2013.791344

Kelly, J. R., and Scheibling, R. E. (2012). Fatty acids as dietary tracers in benthic food webs. *Mar. Ecol. Prog. Ser.* 446, 1–22. doi: 10.1007/s11356-018-2302-x

Li, Y., Ghasemi Naghdi, F., Garg, S., Adarme–Vega, T. C., Thurecht, K. J., Ghafor, W. A., et al. (2014). A comparative study: the impact of different lipid extraction methods on current microalgal lipid research. *Microb. Cell Fact.* 13:14. doi: 10.1186/1475-2859-13-14

MacDonald, J. D. (1869). On the structure of the diatomaceous frustule, and its genetic cycle. *Ann. Mag. Nat. Hist.* 3, 1–8. doi: 10.1080/00222936908695866

MacIntyre, H. L., Geider, R. J., and Miller, D. C. (1996). Microphytobenthos: the ecological role of the secret garden of unvegetated, shallow-water marine habitats. I. Distribution, abundance and primary production. *Estuaries* 12, 186–201. doi: 10.2307/1352224

Mann, D. G. (1993). Patterns of sexual reproduction in diatoms. *Hydrobiologia* 26, 11–20. doi: 10.1007/bf00027999

Mann, D. G. (2011). "Size and Sex, in The Diatom World. Cellular Origin, Life," in *Extreme Habitats and Astrobiology*, Vol. 19, eds J. Seckbach and P. Kociolek (Netherlands: Springer), 145–166. doi: 10.1007/978-94-007-1327-7_6

Mann, D. G., and Stickle, A. J. (1991). The genus *Craticula*. *Diatom Res.* 6, 79–107. doi: 10.1080/0269249X.1991.9705149

McGinnis, K. M., Dempster, T. A., and Sommerfeld, M. R. (1997). Characterization of the growth and lipid content of the diatom *Chaetocores muelleri*. *J. Appl. Phycol.* 9, 19–24.

Mizuno, M. (1994). Sexual reproduction and auxospore formation in *Achnanthes javanica* f. *subconstricta*. *Diatom Res.* 9, 133–141.

Mizuno, M., and Okuda, K. (1985). Seasonal change in the distribution of cell size of *Cocconeis scutellum* var. *ornata* (Bacillariophyceae) in relation to growth and sexual reproduction. *J. Phycol.* 21, 547–553. doi: 10.1111/j.0022-3646.1985.00547.x

Mohan, N., Rajaram, M. G., Baskara Boopathy, A., and Rengasamy, R. (2012). Biomass and lipid production of marine diatom *Amphiprora paludosa* W. *J. Algal Biomass Utln.* 3, 52–59.

Natana Murugaraj, G., and Jeyachandran, S. (2007). Effect of salinity stress on the marine diatoms *Amphora coffeaeformis* (Ag.) Kuetz.

(Bacillariophyceae) in relation to proline accumulation. *Seaweed Res. Utln.* 29, 227–231.

Pernet, F., Tremblay, R., Demers, E., and Roussy, M. (2003). Variation of lipid class and fatty acid composition of *Chaetoceros muelleri* and *Isochrysis* sp. grown in a semicontinuous system. *Aquaculture* 221, 393–406.

Pfitzer, E. (1869). Über Bau und Zellteilung der Diatomeen. *Bot. Zeitung* 27, 774–776.

R Core Team (2020). *R: A language and Environment for Statistical Computing*. Austria: R Foundation for Statistical Computing.

Renaud, S. M., Thinh, L. V., Lambrinidis, G., and Parry, D. L. (2002). Effect of temperature in growth, chemical composition and fatty acid composition of tropical Australian microalgae in batch cultures. *Aquaculture* 211, 195–214. doi: 10.1016/s0044-8486(01)00875-4

Round, F. E., Crawford, R. M., and Mann, D. G. (1990). *The Diatoms. Biology and Morphology of the Genera*. Cambridge, UK: Cambridge University Press, 233–235.

Schneider, C. A., Rasband, W. S., and Eliceiri, K. W. (2012). NIH Image to ImageJ: 25 years of image analysis. *Nat. Methods* 9, 671–675. doi: 10.1038/nmeth.2089

Sherr, E., and Sherr, B. (2007). Heterotrophic dinoflagellates: a significant component of microzooplankton biomass and major grazers of diatoms in the sea. *Mar. Ecol. Prog. Ser.* 352, 187–197.

Smol, J. P., and Stoermer, E. F. (2010). *The Diatoms: Applications for the Environmental and Earth Sciences, second ed*. Cambridge, UK: Cambridge University Press, 1–667.

Svenning, J. B., Dalheim, L., Vasskog, T., Matricon, L., Vang, B., and Olsen, R. L. (2020). Lipid yield from the diatom *Porosira glacialis* is determined by solvent choice and number of extractions, independent of cell disruption. *Sci. Rep.* 10:22229. doi: 10.1038/s41598-020-79269-z

Wood, A. M., Everroad, R. C., and Wingard, L. M. (2005). "Measuring growth rates in microalgal cultures," in *Algal Culturing Techniques*, ed. R. A. Andersen (London, UK: Elsevier), 269–286. doi: 10.1016/b978-012088426-1/50019-6

Wu, S., Zhang, B., Huang, A., Huan, L., He, L., Lin, A., et al. (2014). Detection of intracellular neutral lipid content in the marine microalgae *Prorocentrum micans* and *Phaeodactylum tricornutum* using Nile red and BODIPY 505/515. *J. Appl. Phycol.* 26, 1659–1668. doi: 10.1007/s10811-013-0223-0

Zheng, W., Chen, C., Wang, Y., Bao, K., Wang, X., and Chu, C. (2005). Effects of potassium iodide on the growth and metabolite ac-cumulation of two planktonic diatoms. *J. Appl. Phycol.* 17, 355–362.